Carcinogenesis vol.30 no.4 pp.589–597, 2009
doi:10.1093/carcin/bgp036
Advance Access publication January 30, 2009

Tissue-resident stem cells promote breast cancer growth and metastasis

Fabian L.Muehlberg[†], Yao-Hua Song[†], Alexander Krohn, Severin P.Pinilla, Lilly H.Droll, Xiaohong Leng, Max Seidensticker[1], Jens Ricke[1], Andrew M.Altman, Eswaran Devarajan, Weili Liu, Ralph B.Arlinghaus and Eckhard U.Alt[*]

Department of Molecular Pathology, University of Texas M. D. Anderson Cancer Center, Houston, TX 77030, USA and [1]Clinic for Diagnostic Radiology, University Hospital, Otto-von-Guericke University, Magdeburg 39120, Germany

[*]To whom correspondence should be addressed. University of Texas M.D. Anderson Cancer Center, SCRB2, Box 951, 7435 Fannin Street, Houston, TX 77054, USA. Tel: +713 834 6117; Fax: +713 834 6083;
Email: ealt@mdanderson.org
Correspondence may also be addressed to Yao-Hua Song.
Email: ysong@mdanderson.org

Mesenchymal stem cells derived from bone marrow have recently been described to localize to breast carcinomas and to integrate into the tumor-associated stroma. In the present study, we investigated whether adipose tissue-derived stem cells (ASCs) could play a role in tumor growth and invasion. Compared with bone marrow-derived cells, ASCs as tissue-resident stem cells are locally adjacent to breast cancer cells and may interact with tumor cells directly. Here, we demonstrate that ASCs cause the cancer to grow significantly faster when added to a murine breast cancer 4T1 cell line. We further show that breast cancer cells enhance the secretion of stromal cell-derived factor-1 from ASCs, which then acts in a paracrine fashion on the cancer cells to enhance their motility, invasion and metastasis. The tumor-promoting effect of ASCs was abolished by knockdown of the chemokine C-X-C receptor4 in 4T1 tumor cells. We demonstrated that ASCs home to tumor site and promote tumor growth not only when co-injected locally but also when injected intravenously. Furthermore, we demonstrated that ASCs incorporate into tumor vessels and differentiate into endothelial cells. The tumor-promoting effect of tissue-resident stem cells was also tested and validated using a human breast cancer line MDA-MB-231 cells and human adipose tissue-derived stem cells. Our findings indicate that the interaction of local tissue-resident stem cells with tumor stem cells plays an important role in tumor growth and metastasis.

Introduction

It has been increasingly recognized that cancer cells actively recruit stromal cells into the tumors and that this recruitment is essential for the generation of a microenvironment that promotes tumor growth (1–4). The presence of a large number of myofibroblasts is apparent in the stromal compartment of most invasive human breast cancers but not found in the stroma of normal breast tissue (5). Myofibroblasts are stromal fibroblasts with features of both myoblasts [e.g. expression of smooth muscle actin (SMA)] and fibroblasts that have been implicated in breast cancer invasion, extracellular matrix remodeling, wound healing and chronic inflammation (6). The cell type of origin of myofibroblasts is not conclusively established. Isolation of various stromal and epithelial cells from breast tumors and their coculturing *in vitro* demonstrated that cancer epithelial cells can induce the expression of myofibroblast markers in a subset of fibroblasts (7). However, the finding that only a small fraction of fibroblasts were transformed into myofibroblasts (7) raises the question of whether myofibroblasts could be derived from specific stem cells that are recruited by cancer epithelial cells from either bone marrow or locally in the adjacent breast adipose tissue. Recent data both in animal models and human breast tumors support the hypothesis that at least a subset of cancer-associated myofibroblasts is derived from circulating bone marrow-derived cells (8,9). It has been shown that adipose tissue also contains pluripotent mesenchymal stem cells (10). In the present study, we set out to determine whether and how adipose tissue-derived stem cells (ASCs) could be involved in promoting tumor growth and metastasis.

Abbreviations: ASC, adipose tissue-derived stem cell; CT, computed tomography; CXCR, chemokine C-X-C receptor; EC, endothelial cell; FBS, fetal bovine serum; GFP, green fluorescent protein; i.v., intravenously; mASC, murine adipose tissue-derived stem cell; RANTES, regulated on activation, normal T-cell expressed and secreted; SDF-1, stromal cell-derived factor-1; SMA, smooth muscle actin; VEGF, vascular endothelial growth factor; vWF, von Willebrand factor.

[†]These authors contributed equally to this work.

Materials and methods

Cell lines and cell culture techniques

4T1 cells were purchased from American Type Culture Collection (ATCC, Manassas, VA) and cultured in RPMI 1640 medium from Cellgro (Manassas, VA) supplemented with 10% heat-inactivated fetal bovine serum (FBS) (Atlanta Biologicals, Lawrenceville, GA), 2 mM glutamine, 100 U/ml penicillin and 100 μg/ml streptomycin. 4T1 mammospheres have been selected by culturing in a defined serum-free medium (Dulbecco's modified Eagle's medium–F12) that is supplemented with 2% B-27 (Invitrogen, Carlsbad, CA), 40 ng/ml recombinant human fibroblast growth factor basic (bFGF) (Chemicon, Billerica, MA), 100 ng/ml thrombin (R&D Systems, Minneapolis, MN), 20 ng/ml epidermal growth factor, 1 mM 2-mercaptoethanol, 1 ng/ml leukemia inhibiting factor and 1% insulin transferin sodium selenite (ITS) (Sigma, St. Louis, MO).

Isolation of murine adipose tissue-derived stem cell

Ten Balb/c mice were killed by cervical dislocation. Perirenal, pelvine and subcutaneous fat tissue were dissected from mice, washed in phosphate-buffered saline and immediately processed. After mincing the tissue in pieces <2 mm^3, serum-free α-modified Eagle medium (1 ml/1 g tissue) and 2 U/g tissue Liberase Blendzyme 3 (Roche Diagnostics, Indianapolis, IN) was added and incubated under continuous shaking at 37°C for 45 min. The digested tissue was sequentially filtered through 100 and 40 μm filters (Fisher Scientific, Pittsburgh, PA) and centrifuged at 450*g* for 10 min. The supernatant containing adipocytes and debris was discarded, and the pelleted cells were washed twice with Hanks' balanced salt solution (Cellgro) and finally resuspended in growth media. Growth media contained alpha-modification of Eagle's medium (Cellgro), 20% FBS (Atlanta Biologicals), 2 mM glutamine (Cellgro) and 100 U/ml penicillin with 100 μg/ml streptomycin (Cellgro). Plastic-adherent cells were then grown in Nunclon culture vials (Nunc, Rochester, NY) at 37°C in a humidified atmosphere containing 5% CO_2 followed by daily washes to remove red blood cells and non-attached cells. After 80% confluence of passage 0, cells were seeded at a density of 3000 cells/cm^2 (passage 1).

Migration assay

The Fluoroblok Transwell Migration System (BD Biosciences, Bedford, MA) with 3 μm pore size was used for migration experiments. 4T1 cells (3×10^4) were plated in the upper chamber of a 3 μm transwell system. The lower chamber was filled with 1 ml of 72 h conditioned medium of mASC. After 24 h of migration through the transwell membrane, cells were fixed and stained with calcein. For blocking of CXCR4, a neutralization antibody was used (R&D Systems) at a concentration of 30 μg/ml 1 h before and during the migration assay.

Invasion assay

The chemoinvasion assay was performed using Boyden chambers with filter inserts (pore size, 8 μm) coated with Matrigel in 24-well dishes (BD Biosciences) as described previously (1). The 4T1 and ASCs (3×10^4 cells and 6×10^4 cells, respectively) were placed in 600 μl of 5% FBS containing modified Eagle medium in the upper chamber, and 750 μl of the same medium containing 10% FBS was placed in the lower chamber. The plates were incubated for 48 h at 37°C in 5% CO_2. Cells on the upper side of the filters were removed with cotton-tipped swabs, and the filters were washed with phosphate-buffered saline. Cells on the underside of the filters were

examined and counted under a microscope. Green fluorescent cell signal of green fluorescent protein (GFP)-labeled 4T1 cells was counted in five randomly chosen view fields at a 5-fold magnification of every insert. Each experiment was repeated at least three times.

mASC GFP labeling

Stable GFP labeling was performed with a third-generation lentivirus system as described previously by our group (11).

CXCR4 knockdown

CXCR4 expression was diminished in 4T1 cells by transfection with a third-generation lentivirus containing short hairpin RNA construct against CXCR4 coding sequence as described previously by our group (12).

Quantitative real-time polymerase chain reaction analysis of gene expression

Reverse transcription–polymerase chain reaction was used to quantify CXCR4 messenger RNA levels following reverse transcription as described previously by our group (12). Primers used for the detection of CXCR4 were 5′-TCCAACAAGGAACCCTGCTTC-3′ (forward primer) and 5′-TTGCCGACTATGCCAGTCAAG-3′ (reverse primer) (amplicon 122 bp) and for GAPDH 5′-TGGCAAAGTGGAGATTGTTGCC-3′ (forward primer) and 5′-AAGATGGTGATGGGCTTCCCG-3′ (reverse primer) (160 bp).

Enzyme-linked immunosorbent assay for stromal cell-derived factor-1/vascular endothelial growth factor

The enzyme-linked immunosorbent assay was performed using the mouse CXCL12/SDF-1 and VEGF Quantikine Kit (R&D Systems) as per the manufacturer's instruction. Medium was conditioned over 72 h, centrifuged and filtered through a 0.45 μm Steriflip Filter Unit (Millipore, Billerica, MA). The amount of stromal cell-derived factor-1 (SDF-1) was normalized to DNA content (nanogram SDF-1 per microgram DNA). DNA isolation was performed using DNeasy Blood & Tissue Kit (Qiagen, Valencia, CA) following manual instructions.

Western blot analysis

Cells were lysed in radial immunoprecipitation assay lysis buffer (Upstate, Billerica, MA), including protease inhibitor cocktail (Roche Diagnostics), and westernblot was performed as we have described previously (13).

Animal experiments

Thirty nude male Balb/c mice in the age of 6–8 weeks were injected with 5×10^3 4T1 spheroid-forming cells subcutaneously into the inguinal mammary fat pad number four. Tumor measurements every fifth day was carried out by caliper. At day 21, post-injection mice were scanned by high-resolution micro-computed tomography (CT) under anesthesia with 2–3% isoflurane.

For SDF-1 measurements in mASCs of cancer mice, fat tissue around the tumor-infiltrated mammary fat pad was dissected. Contamination of this culture by cancer cells was minimized by using of GFP-labeled 4T1 mammospheres for tumor induction and following fluorescence-activated cell sorting for GFP-negative cells after dissection of tissue.

Tumor digestion

After dissecting the tumors, tissue was minced quickly with scalpels into fragments <2 mm^3. Digestion into single-cell suspension was performed using an enzyme mix containing 12 500 U collagenase II and IV (Sigma–Aldrich) in 20 ml serum-free media under 37°C for 35 min. Suspension was then filtered through a 70 μm nylon mesh and red blood cells were finally removed by centrifugation with Ficoll for 10 min at 300*g*. Fluorescence-activated cell sorting for GFP-positive cells was performed immediately afterward without any further *in vitro* culture.

Flow cytometry

Cells were incubated with antibodies against von Willebrand Factor (vWF) and alpha-SMA and the percentage of positive cells analyzed by flow cytometry as described previously by our group (14).

MicroCT imaging

CT scans were made using GE Healthcare Enhanced Vision System. Scan parameters: tube voltage 80 kV, anode current 470 μA, number of views 360, exposure time 600 ms, detector bin mode 2×2, effective pixel size 0.046 mm. Fenestra™ vascular contrast solution (ART Advanced Research Technologies, Alfred Nobel, St. Laurent, QC, Canada) was injected into tail veins 2 h prior to CT scans. Anesthesia was induced using 5% isoflurane and maintained with 1–2% isoflurane. Image review was performed at a Vitrea© workstation (Vital Images, Minnetonka, MN). The size of the primary tumor was obtained in x, y and z axis. Calculation of the tumor volume was performed by employing the spherical volume equation $V = \frac{4}{3} \times \pi \times r_x \times r_y \times r_z$. Vascularity of the tumors was assessed by measuring the average Hounsfield units of a region of interest (ROI) that was always excluding the central necrosis if present. As an intraindividual reference, the density (Hounsfield unit) of a ROI of thigh musculature was obtained.

Immunohistochemical staining and capillary density

Immunostaining was performed using tumor sections using antibody against vWF and vascular density was determined as described previously by our group (15).

Results

Isolation and characterization of 4T1 mammospheres

Spheroid-forming cells are cancer-initiating cells. Cancer-initiating cells have been found in both breast cancer lesions and from an established breast carcinoma cell line (16–18). In an elegant study, human mammary epithelial cells were used to generate non-adherent spheroids (designated mammospheres) in cell culture and demonstrate the presence of the three mammary cell lineages. More importantly, the cells in the mammospheres were clonally derived, providing evidence for a single pluripotent stem cell (19). To enrich the small subpopulation of cancer-initiating cells, we used the selection method developed in our lab by culturing the 4T1 cells in a special serum-free medium (containing bFGF/epidermal growth factor/leukemia inhibiting factor) for 7 days. The selection method is based on the fact that the condition of the medium allows cancer progenitor cells (also called cancer-initiating or cancer stem cells) to form spheroids but does not allow regular cancer cells to grow. After 24 h of culture, the cells start to form sphere-like bodies that appear as non-adherent or only partially adherent (Figure 1). Normally, at least 4000 regular 4T1 cells are required to induce tumor in mice. However, the

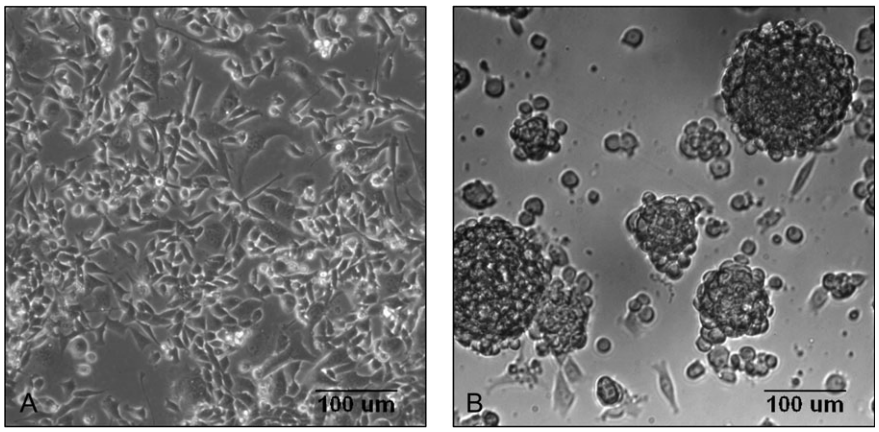

Fig. 1. (**A**) Unselected adherent 4T1 breast cancer cells in 10% FBS/RPMI; (**B**) 4T1 spheroid-forming cells after 72 h selection in our special serum-free medium.

injection of only 100 spheroid-derived cells into eight nude Balb/c mice resulted in tumor formation in all cases (data not shown) suggesting a remarkable tumor initiation potential and thereby making our results more comparable as far as the initiation of tumor formation is concerned. Unless indicated differently, those spheroid-forming 4T1 cells (4T1 mammospheres) were used in the subsequent studies.

Adipose tissue-derived stromal cells

The stromal cells used in this study are not adipocytes. There is a growing body of experimental evidence from both *in vitro* and *in vivo* studies demonstrating the multipotency of ASCs from adipose tissue isolated from humans and other species. These include the differentiation potential into adipocyte (10,20–22), chondrocyte (10,20,23,24), hematopoietic supporting cells (25,26), hepatocyte (27,28), neuronal-like cells (20,29–31), osteoblast (10,20,32,33), pancreatic (34) and skeletal myocyte (10,20,35), vascular cell (15) and cardiomyocyte pathways (36). The phenotypes of ASCs have been characterized previously (14). Briefly, ASCs are positive for CD44 (99.36 ± 0.75%), CD90 (97.59 ± 2.45%) and CD105 (98.51 ± 1.83%) and negative for CD11b (0.33 ± 0.18%), CD14 (0.51 ± 0.11%), CD34 (1.09 ± 0.16%), CD45 (0.39 ± 0.29%) and HLA-DR (0.68 ± 0.92%). Clonal expansion studies have shown that ASCs are capable of differentiating into all three lineages (X.Bai, Y.Song, E.Alt, submitted for publication).

Migration of 4T1 breast cancer cells and 4T1 mammospheres toward ASCs

mASCs were isolated from the perirenal and pelvine fat tissue of 10 immunocompetent Balb/c mice. Conditioned medium was collected from mASCs after 72 h in culture.

Using an *in vitro* transwell migration assay, we demonstrated that 4T1 breast cancer cells migrate toward the conditioned medium of mASC (Figure 2A). Interestingly, 4T1 mammospheres show a significantly higher number of migrating cells (∼40%) compared with unselected adherent 4T1 cells.

SDF-1/CXCR4 axis is mainly responsible for migration of 4T1 cells and 4T1 mammospheres toward mASC

It has been shown that SDF-1 plays an important role in tumor growth and metastasis (37). In this study, we found that mASC secrete elevated levels of SDF-1, whereas 4T1 cells express CXCR4 which is the receptor for SDF-1 (Figure 2B). Interestingly again, 4T1 mammosphere cells have significantly higher messenger RNA levels of the CXCR4 receptor compared with their unselected counterparts or to mASC.

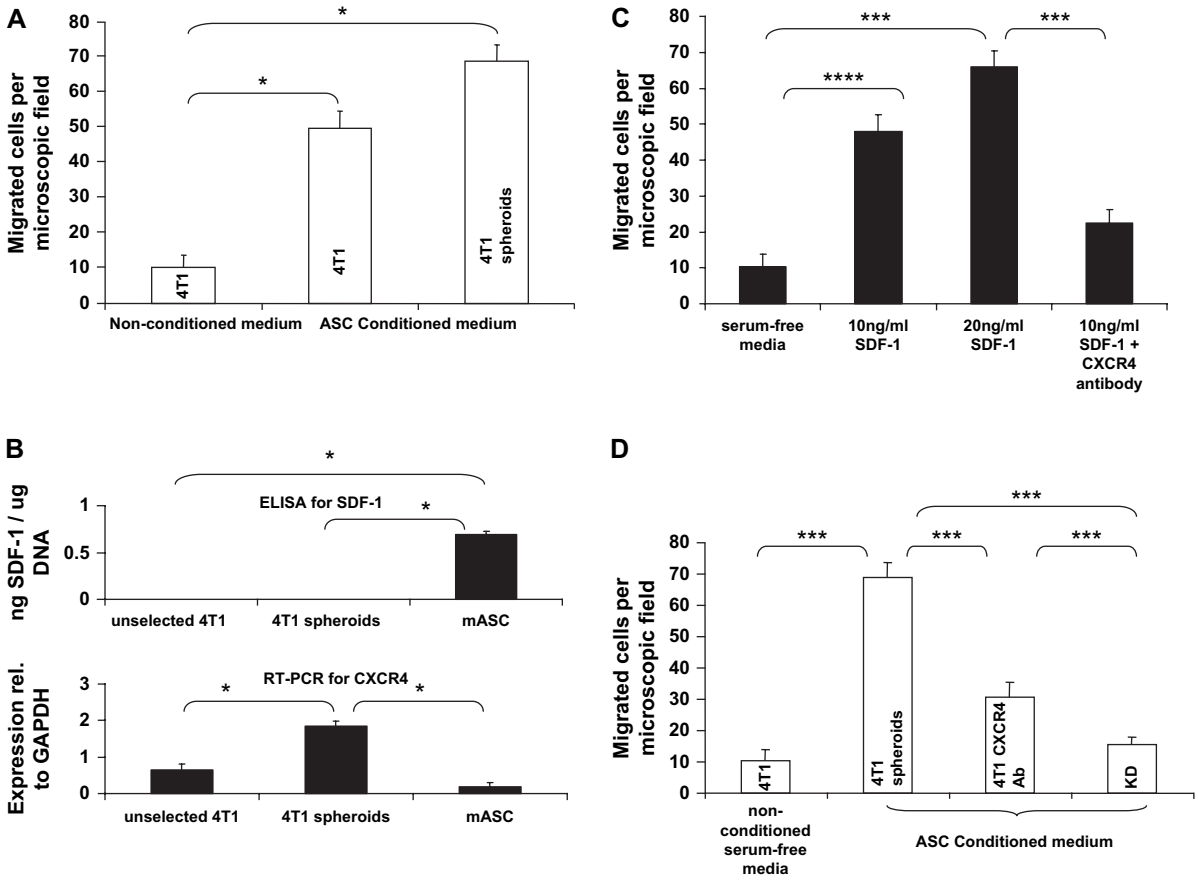

Fig. 2. (**A**) 4T1 cells and especially spheroid-forming 4T1 cells migrate toward the conditioned medium of mASC. 4T1 cells (3×10^4) were plated in the upper chamber of a 3 μm transwell system. The lower chamber was filled with 1 ml of 72 h conditioned medium of mASC. After 24 h of migration through the transwell membrane, cells were fixed and stained with calcein. The results are the mean and SD number of migrated cells per microscopic field under fluorescent microscope. Background: regular 4T1 cells on upper chamber and the lower chamber contains non-conditioned serum-free medium; 4T1: regular 4T1 cells on upper chamber and conditioned serum-free medium from the ASCs; 4T1 spheroids: 4T1 spheroid-forming cells on top and conditioned serum-free medium from ASC on the bottom. (**B**) mASC but not 4T1 cells produce SDF-1; 4T1 cells especially spheroid-forming 4T1 cells show higher messenger RNA levels of the specific receptor CXCR4. Secreted amounts of SDF-1a were measured by enzyme-linked immunosorbent assay and CXCR4 messenger RNA levels were determined by quantitative reverse transcription–polymerase chain reaction (RT–PCR). Reverse transcription–polymerase chain reaction results were normalized against GAPDH. (**C**) 4T1 cells and mammospheres migrate toward recombinant SDF-1. A total of 3×10^4 4T1 spheroid-forming cells were plated in the upper chamber of a 3 μm transwell system. Recombinant murine SDF-1 in serum-free medium was filled into the lower chamber in stated concentrations. CXCR4 inhibition was performed by 30 μg/ml neutralizing antibody 1 h before and during the migration assay. (**D**) 4T1 migration toward mASC conditioned medium is mediated mainly by SDF-1. $^{*}P < 0.05$, $^{***}P < 0.001$, $^{****}P < 0.001$.

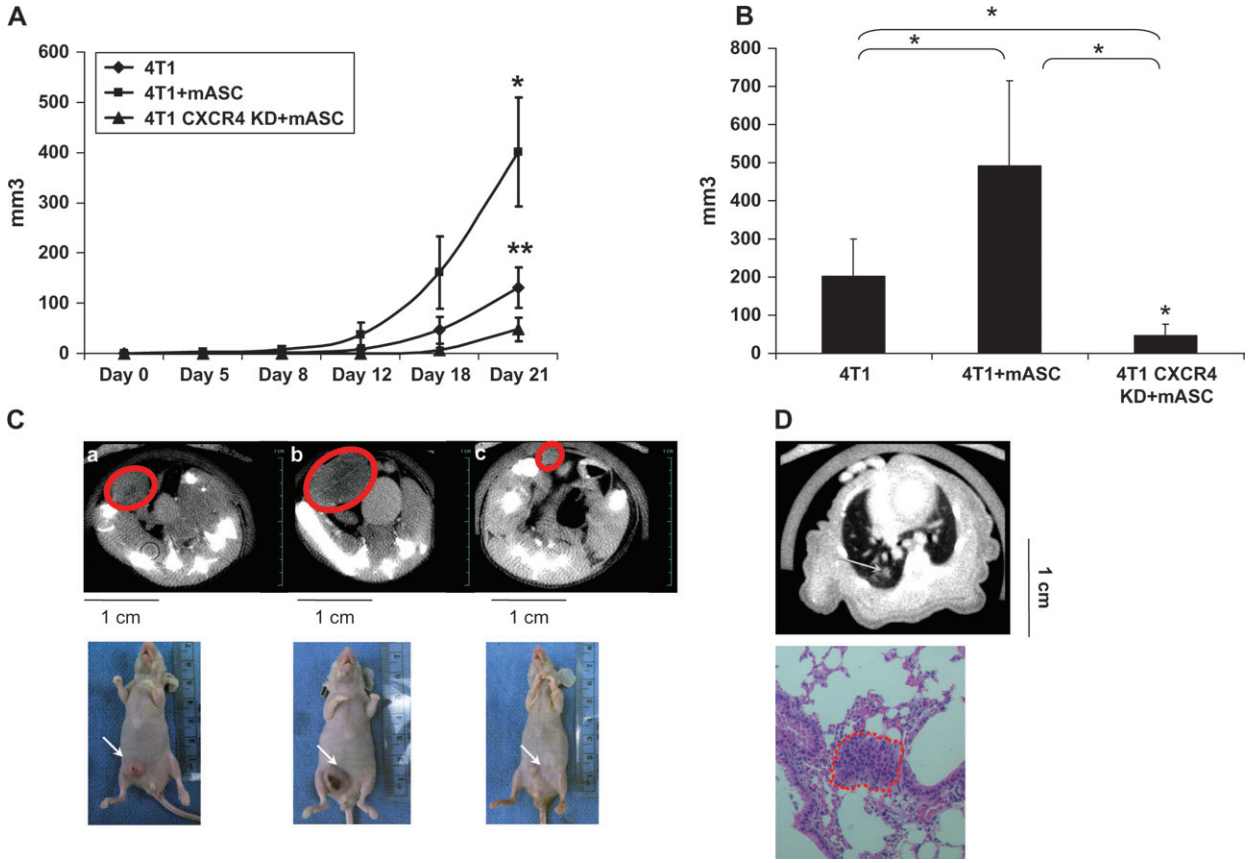

Fig. 3. (**A**) Tumor growth is enhanced when 4T1 spheroid-forming cells are co-injected with mASC. A total of 5×10^3 4T1 spheroid-forming cells or spheroid-forming cells with CXCR4 knockdown, respectively, were injected or co-injected with 5×10^4 GFP-labeled mASC subcutaneously. Values represent volume measurements (mm^3) with scientific caliper. (**B**) Tumor volume 21 days post-injection is increased when 4T1 spheroid-forming cells are co-injected with mASC and decreased using 4T1 cells with CXCR4 knockdown. Columns represent tumor volumes in mm^3 ± SDs evaluated from microCT images at day 21. (**C**) The respective microCT images show sections of tumors (upper panel) correspond to photographic images of tumors *in situ* (lower panels), (**a**) 5×10^3 4T1 only, (**b**) 5×10^3 4T1 + 5×10^5 GFP-mASC and (**c**) 5×10^3 4T1 CXCR4 KD + 5×10^4 GFP-mASC. (**D**) Macroscopic and microscopic-sized lung metastasis: microCT image (upper picture). Arrow shows lung metastasis in a mouse co-injected with 4T1 spheroid-forming cells and mASC on day 21 post-injection. Hematoxylin and eosin staining of paraffin-embedded lung section from mouse from stem cell group (lower picture). *4T1 + mASC versus 4T1, $P < 0.05$; **4T1 versus 4T1 CXCR4 KD + mASC, $P < 0.01$.

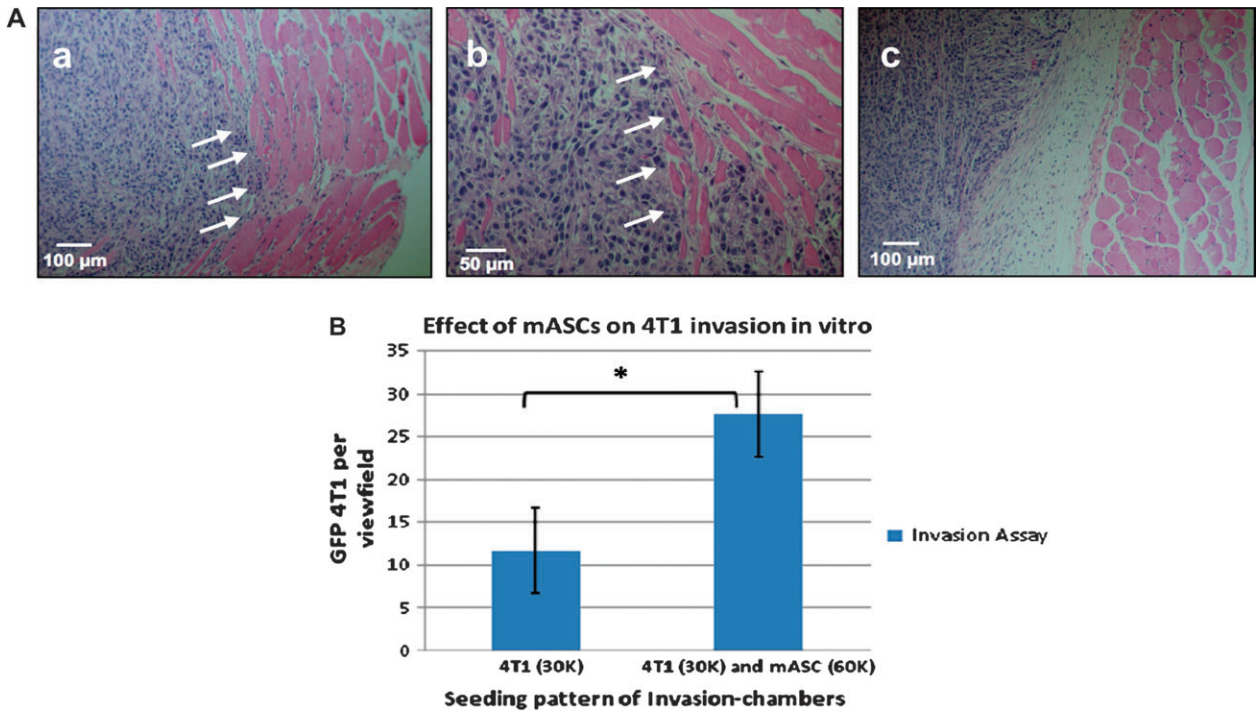

Our data showed that recombinant SDF-1 triggers migration of 4T1 spheroid-forming cells (Figure 2C).

To determine whether the SDF-1/CXCR4 axis would be crucial for the observed differences in migration, we studied the effects by both a knockdown of CXCR4 in 4T1 mammospheres using a lentiviral short hairpin RNA construct and by receptor inhibition with a neutralizing antibody. As shown in supplementary Figure 1 (available at *Carcinogenesis* Online), CXCR4 short hairpin RNA substantially suppressed CXCR4 protein expression by western blot analysis.

Both the CXCR4 knockdown and receptor neutralization led to a significant decrease in migration of 4T1 mammospheres toward mASC conditioned medium suggesting a pivotal role of SDF-1 in initiation of this migratory effect (Figure 2D).

mASC promote tumor growth in vivo when injected together with 4T1 mammospheres

In order to find out whether mASC promotes tumor growth and metastasis, we injected 5×10^3 4T1 mammospheres in one group and 5×10^3 4T1 mammospheres together with 5×10^4 GFP-labeled mASC in another group of 10 nude Balb/c mice each subcutaneously into the mammary fat pad. Tumor volumes were measured by scientific caliper (Figure 3A). After 3 weeks, microCT scans (Figure 3B) were performed in order to determine exact final tumor volumes and to locate metastasis.

Tumors in mice injected with 4T1 mammospheres and mASC formed a macroscopic visual tumor earlier (10/10 five days after injection) than the group only injected with 4T1 mammospheres (6/10 five days after injection and 10/10 after 12 days) (Figure 3A). Tumor growth rates were also significantly higher in the co-injection group (0.44 mm/day average increase in diameter) compared with mice only injected with mammospheres (0.3 mm/day average increase in diameter). At the time of microCT scans (day 21 post-injection), the average tumor volume of mice injected with 4T1 mammospheres together with mASC was 490.8 mm^3 (±225 mm^3), whereas tumors in the 4T1 group without ASCs only measured 202 mm^3 (±98 mm^3) in average (Figure 3B).

In order to further investigate if our *in vitro* findings of SDF-1 serving as a chemoattractant for 4T1 cells would be of relevance also *in vivo*, we co-injected 5×10^4 mASC and 5×10^3 4T1 mammospheres with a CXCR4 knockdown into another group of 10 mice. The tumors formed in this group developed significantly later (0/10 at day 5, 2/10 at day 8 and 8/10 at day 12) and grew less fast with 0.21 mm/day average increase in diameter compared with the other groups (Figure 3A). When killed, the average tumor size was 47 mm^3 (±28.8 mm^3). This represents a 76.7 and 90.4% reduction in tumor size compared with 4T1-alone group and 4T1 plus mASC group, respectively (Figure 3B). Representative images of tumor size from the three groups are shown in Figure 3C.

Metastasis into the lungs is blocked by CXCR4 knockdown and increased when mASC are co-injected with 4T1 mammospheres

High-resolution microCT images of the thoracic, abdominal and pelvine body parts of the mice were diligently analyzed by our radiologists in order to detect metastasis—especially in the lungs (Figure 3D). In the 4T1 group without ASCs ($n = 10$), three mice were free of lung metastases and only moderate numbers of lung metastases were found in the remaining mice. Nine of the 10 mice in the stem cell co-injection group showed multiple lung metastases. In contrast, only four mice in the knockdown group ($n = 9$) showed single small-sized metastasis in the lung, suggesting that the SDF-1/CXCR4 axis is essential not only to the growth of the primary tumor but also for its ability to metastasize.

In order to find out whether ASCs produce more SDF-1 under the influence of the tumor microenvironment, we injected 1.5×10^4 GFP-labeled 4T1 mammospheres into the mammary fat pad of five nude Balb/c mice. Another five mice have been injected with 20 µl phosphate-buffered saline serving as a control group. After 2 weeks, tumors have formed in mice injected with 4T1 mammospheres (average tumor diameter 7.2 mm ± 0.98 mm), mice were killed and the mASCs were isolated from fat tissue surrounding the tumor. mASC isolated from these cancer mice showed an increase of SDF-1 release (supplementary Figure 2 is available at *Carcinogenesis* Online).

To determine whether ASCs could differentiate into cancer-associated fibroblasts or myofibroblast, we dissected out the tumor and prepared single-cell suspension and quantified SMA-positive cells. Our data showed that the ASCs express 42.47 ± 1.42% SMA before injection and this number increased to 57.03 ± 3.01% in ASCs isolated from tumors ($P < 0.01$).

Tumor growth in the knockdown group resembled symmetrical spherical growth with an exact tumor margin, whereas the 4T1 group and moreover the stem cell group plus 4T1 showed distorted spherical symmetries, invasive growth patterns, coarse tumor margins and satellite structures. Hematoxylin and eosin staining of tumor margins confirms the invasive growth patterns into the surrounding abdominal skeletal muscles in the 4T1 (Figure 4Aa) and stem cell group (Figure 4Ab), whereas the CXCR4 knockdown in 4T1 cells leads to a partial encapsulation of the primary tumor (Figure 4Ac).

In order to determine whether 4T1 tumor cells become more invasive in the presence of ASCs, we performed an invasion assay in a Boyden chamber. As shown in Figure 4B, ASCs promote the invasion of 4T1 cells when mixed with tumor cells at the ratio of 2:1 (ASC:4T1).

Vascularity and capillary density are enhanced by mASC

Vascularization of the tumor as determined by the Houndsfield unit value of the tumor relative to the musculature evaluated from microCT images showed higher vascularity in the 4T1/mASC group compared with the 4T1 group (Figure 5A). The 4T1 CXCR4 KD/mASC group features lower enhancement and accordingly a decreased vascularity of the corresponding tissue.

These image-derived data are supported by the capillary density as assessed from frozen sections by fluorescent staining for vWF. As illustrated in Figure 5B, tumor sections out of the stem cell co-injection group show a higher number of capillaries per microscopic field (20.6 ± 1.9) than those from the 4T1 group (12.25 ± 2.2) and the CXCR4 knockdown group (8.75 ± 1.6). Our data also showed that ASCs are incorporated into tumor vessels (Figure 5C, green) and some of them colocalized with vWF staining (Figure 5C and D, yellow) indicating differentiation of mASCs into endothelial cells (ECs).

Vascular endothelial growth factor (VEGF) plays an important role in tumor-induced neoangiogenesis. Our data demonstrate that 4T1 spheroid-forming cells secrete high levels of VEGF (104.8 ± 7.4 pg/10^6 cells/24 h) that is significantly reduced in 4T1 spheroid-forming cells with CXCR4 knockdown (46.4 ± 2.53 pg/10^6 cells/24 h) (supplementary Figure 3 is available at *Carcinogenesis* Online).

In order to find out if ASCs could differentiate into vascular ECs to support neoangiogenesis, we dissected the tumors and dissociated into a single-cell suspension and cell populations of vWF were quantified. Our data show that before injection, ASCs that are positive for vWF is

Fig. 4. CXCR4 knockdown blocks invasive growth patterns. Hematoxylin and eosin-stained paraffin-embedded sections of tumor margin are shown in these figures. (**A**) Invasive growth of cells from primary tumor infiltrating the surrounding skeletal muscles of the abdominal wall can be observed in the group injected with 4T1 (**a**) and co-injection group (4T1 + mASC) (**b**). Knockdown of CXCR4 (**c**) results in tumor sites without invasive growth patterns and tumor appears encapsulated. 4T1 tumor cells become more invasive in the presence of ASCs. (**B**) Cell lines were seeded alone or in a 1:2 ratio (4T1:mASC). The upper chamber contained 5% FBS and the lower contained 10% FBS in all invasion assays. Inserts were incubated for 48 h and the green fluorescent signals of GFP-labeled 4T1 cells were counted in five randomly chosen view fields per insert. The left column shows the Matrigel membranes before scrubbing the surface with a cotton swab. $^*P \leq 0.005$.

very low (1.84 ± 0.21%). In contrast, 24.1 ± 0.44% of ASCs dissociated from tumors were positive for vWF.

Systemically delivered mASC home to the tumor site and promote tumor growth

In order to determine whether systemic delivery of adipose tissue-derived mesenchymal stem cells could home to tumor site, we injected 3×10^5 GFP-labeled mASC into the tail veins of eight nude Balb/c mice. These mice had been injected with 3×10^4 4T1 spheroid-forming cells 12 h before mASC injections. Subcutaneous injections of 3×10^4 4T1 spheroid-forming cells alone and co-injection of 3×10^4 4T1 spheroid-forming cells together with 3×10^5 GFP-labeled mASC served as control groups. As illustrated in Figure 6A, tumor growth in mice injected with mASC intravenously (i.v.) was enhanced (398 ± 103 mm^3) compared with tumors without mASC injections (198 ± 20 mm^3) ($P < 0.03$) suggesting a supportive effect of mASC following the delivery into the circulatory system. However, mASC directly co-injected with 4T1 cells augmented tumor growth even more (698 ± 60 mm^3).

After killing of mice at day 20 post-injection, tumors were dissected and sectioned. An i.v. injected mASC could be detected inside the tumor by immunostaining for GFP on paraffin-embedded sections (Figure 6B). Furthermore, we were able to show differentiation of our i.v. injected mASC into an endothelial lineage by co-staining for GFP and vWF also in this *in vivo* model (Figure 6C).

In order to assess the number of i.v. injected ASCs recruited into the tumor mass, GFP-positive cells were counted on paraffin sections of tumors i.v. injected with GFP-ASCs and compared with the number of GFP-positive cells in the tumors where GFP-ASC and tumor cells were co-injected by fluorescent microscopy. Tumor samples of comparable size of each group were analyzed in order to minimize possible errors due to different tumor size. As shown in supplementary Figure 4 (available at *Carcinogenesis* Online), approximately one-fifth of i.v. injected ASCs (19.4 ± 2.5%) are found at the tumor site compared with GFP-positive cells in tumors when tumor and ASC cells are co-injected together, suggesting that an active recruitment of systemically delivered ASCs and is in line with tumor growth data (Figure 3A).

In order to determine whether the tumor-promoting effects of adipose tissue-derived stem cells in murine 4T1 models are also valid in other tumor models, we performed a similar study using the MDA-MB-231 human breast cancer model. We injected 5×10^4 MDA-MB 231 cells into a group of 10 nude Balb/c mice and 5×10^4 MDA-MB 231 cells plus 5×10^5 human ASC into another group of 10 mice subcutanously into the inguinal mammary fat pad. There was no tumor formation observable in the group injected with MDA-MB-231 cells alone after three months; whereas six mice in the group co-injected with ASC showed tumor formation within 30 days (supplementary Table 1 is available at *Carcinogenesis* Online), suggesting that the tumor-promoting effect of tissue-resident stem cells is a general phenomenon.

Weinberg's group has recently shown that regulated on activation, normal T-cell expressed and secreted (RANTES) is highly involved in human breast cancer metastasis. We performed additional experiment to investigate whether ASCs also produce RANTES. We were not able to detect RANTES in ASCs or MDA-MB-231 cells when cultured alone; however, we detected significant amount of RANTES in conditioned medium from ASC and MDA-MB-231 cocultures. In order to determine the cellular source of RANTES, we added conditioned medium from MDA-MB-231 cells to ASCs and found significant amount of RANTES produced by ASCs. We also added conditioned medium from ASCs to MDA-MB-231 cells and found no RANTES production. These data suggest that ASCs produce RANTES under the influence of tumor cells.

Discussion

While interactions between adipocytes and breast cancer cells have been described previously (38,39), the involvement of stem cells residing in adipose tissue has not been investigated yet. In this study, we report for the first time that ASCs incorporated into tumor vessels and lead to enhanced tumor growth when co-injected with 4T1 cancer cells. We demonstrated that ASCs home to tumor site when injected i.v. Furthermore, we demonstrate that the SDF-1/CXCR4 axis plays an important role in mediating ASC's tumor-promoting effect.

Our findings that ASCs promote the growth of breast tumor are of special importance since ASCs are derived from adipose tissue that is particularly abundant in breast tissue.

Although ASCs used in the present study were harvested from perirenal and pelvine fat tissue, it has been shown that tissue-resident stem cells are multipotent cells associated with microvessels and are ubiquitously distributed throughout all tissues (40). The results of the present study suggest that in addition to bone marrow-derived cells, local stem cells adjacent to breast cancer cells are involved in tumor growth and metastasis.

SDF-1 has been thought to direct the intratissue localization of tumor cells and to induce metastasis through direct effects on tumor cell migration (41). In line with previous findings (42), our *in vitro* assay showed that 4T1 tumor cells migrate toward conditioned medium of ASCs and that this migration is significantly reduced when the CXCR-4 receptor in 4T1 cells is knocked down.

The mechanisms on how SDF-1 stimulates the outgrowth of established tumors and metastasis are not fully understood yet. In a mouse model of established extrahepatic colorectal metastasis, SDF-1 promoted tumor cell migration *in vitro* and tumor growth of established extrahepatic metastasis *in vivo* due to angiogenesis-dependent induction of tumor cell proliferation and inhibition of apoptotic cell death (43). Furthermore, Brand *et al.* (44) have demonstrated in the colorectal cancer cell line HT-29 that SDF-1 stimulation induces a significant increase in VEGF protein levels. Consistent with these findings, our data show that VEGF level is reduced in 4T1 cells with CXCR4 knocked down. In separate studies, we found that ASCs produce significant amount of insulin-like growth factor-1 (12) and interleukin-6 (S.Pinilla, Y.Song, F.Muehlberg and E.Alt, submitted for publication) that are also involved in tumor growth and metastasis.

Using the Luminex-based Bio-Plex suspension array system, Karnoub *et al.* (4) found that breast cancer cells stimulate *de novo* secretion of RANTES from mesenchymal stem cells, which then acts in a paracrine fashion on the cancer cells to enhance their motility, invasion and metastasis. This enhanced metastatic ability is reversible and is dependent on RANTES signaling through the chemokine receptor CCR5. We demonstrated that ASCs also produce significant amount of RANTES under the influence of cancer cells. These novel findings opened up the possibility of targeting the RANTES-signaling pathway in treating metastatic diseases.

Expression of alpha-SMA is a defining marker for myofibroblast. Orimo *et al.* have shown that fibroblast differentiate into myofibroblast under the influence of the tumor microenvironment. They further demonstrated that myofibroblast but not regular fibroblast produce SDF-1 and promote tumor growth when co-injected with tumor cells. We therefore quantified SMA-positive cells before and after injection. Our data show that 42.47 ± 1.42% of our ASCs express SMA before injection and this number increased to 57.03 ± 3.01% ($P < 0.01$) in ASCs isolated from tumors. Our findings are in line with that of Mishra *et al.* (45) that 17% of bone marrow-derived mesenchymal stem cells express SMA at basal level and this number increased to 89% after exposure to conditioned medium from cancer cells. Our data confirmed the finding by Mishra *et al.* (45) that myofibroblast originate from mesenchymal stem cells; furthermore, our data suggest that tissue resident ASCs are an important source for myofibroblast.

We show that ASCs were not only unable to promote tumor growth when the CXCR4 receptor in 4T1 cells was knocked down but also that the overall tumor size is smaller. Our findings are in line with previous reports. It has been shown that endogenous CXCR4 expression on carcinoma cells correlate with a poor prognosis for several types of carcinomas (46). It is also known that CXCR4 ectopically expressed on carcinoma cells enhances primary tumor growth in a mouse xenograft model (47) and that the knockdown of CXCR4

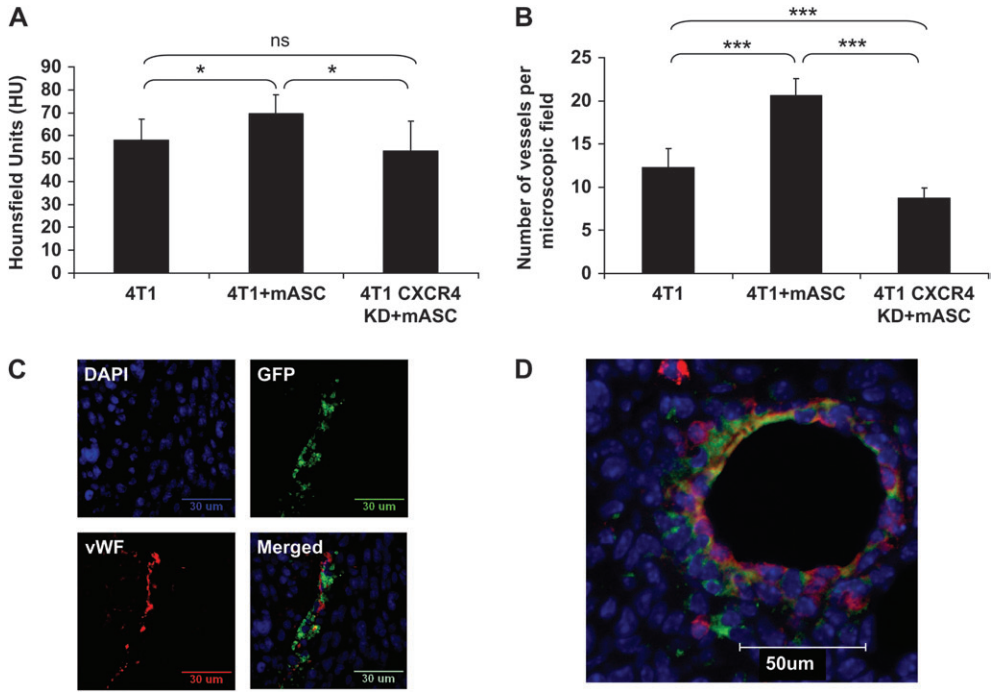

Fig. 5. Vascularity and capillary density are enhanced by mASC. (**A**) Increase of vascularization in stem cell group evaluated from microCT images. Contrast dye injection (Fenestra VC®) 2 h prior to microCT scans on day 21 post-injection facilitated software-supported measuring of vascularization in Hounsfield units by independent radiological core lab (University Magdeburg, Germany). (**B**) Frozen tumor sections were stained for vWF and stained vessels counted under fluorescent microscopy. Each specimen was examined in eight different microscopic fields. Columns represent mean number and SD of capillaries per field. (**C** and **D**): Co-injected GFP-labeled mASC differentiated into ECs. Paraffin-embedded tumor sections from mice injected with 4T1 spheroid-forming cells and GFP-labeled mASC were co-stained with GFP (green) and vWF (red) antibodies. $^{*}P < 0.05$, $^{***}P < 0.001$.

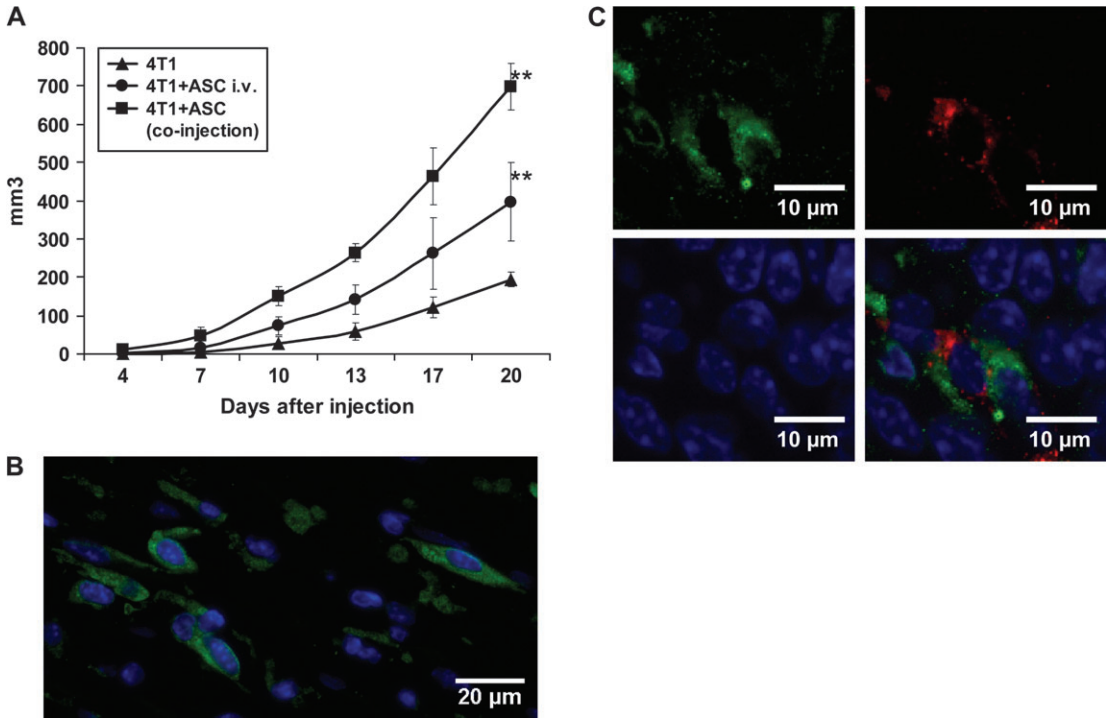

Fig. 6. mASC home to and engraft at tumor site when injected i.v. (**A**) 3×10^4 4T1 spheroid-forming cells were injected into 12 nude Balb/c mice. Eight of those mice were injected with 3×10^5 GFP-mASC i.v. 12 h later. Another group of eight mice was co-injected with 3×10^4 4T1 spheroid-forming cells and 3×10^5 GFP-mASC subcutaneously. Values represent tumor volumes over time evaluated by scientific caliper. (**B**) Paraffin-embedded tumor sections of mice injected with 4T1 spheroid-forming cells and GFP-mASC i.v. stained for GFP and nuclei with 4′,6-diamidino-2-phenylindole (blue) (**C**) Immunostaining of paraffin sections for vWF (red) and GFP (green). 4′,6-Diamidino-2-phenylindole (blue) was used for nucleus staining. $^{**}P < 0.01$.

expression in breast carcinoma cells abrogates the tumor growth (48). Moreover, a small-molecule inhibitor of CXCR4 reduces primary brain tumor growth (49). Thus, it is probably that SDF-1 secreted by ASCs significantly affects CXCR4-expressing 4T1 tumors through direct paracrine stimulation.

Based on observations made nearly 100 years ago that blood vessels grow around tumors (50) and the pioneering work of Folkman (51), it is now widely accepted that tumors must induce angiogenesis in order to grow beyond a size of 1–2 mm in diameter, as well as to metastasize to distant organ sites. The exact mechanisms underlying this tumor-induced neoangiogenesis are still not fully understood. Our findings that GFP-labeled ASCs incorporate into blood vessels within the tumor via direct differentiation into ECs indicate that ASCs contribute to tumor angiogenesis. This observation mirrors previous findings that implanted ASCs differentiated into ECs and SMCs, which incorporated into newly formed vessels in an ischemic injury model (52). We have shown previously that ASCs are multipotent stem cells that have extraordinary proangiogenic potential (11).

However, other mechanisms may also be involved. It has been shown that myofibroblast-derived SDF-1 recruits endothelial progenitor cells into carcinomas, enhancing angiogenesis and thus tumor growth (38). Therefore, ASC-derived SDF-1 may be partially responsible for the increased vascular density observed in our study. Moreover, our finding that ASCs release higher levels of SDF-1 after coculture is in agreement with that of previous reports that myofibroblasts extracted from human mammary tumors express increased levels of the SDF-1 messenger RNA (38). Together, these findings highlight the similarities between tumor stroma formation and wound-healing response.

The aim of our experimental design was to better understand the mechanisms relating to breast cancer growth. Recent studies by others have shown that cancer stem cells were found in both breast cancer lesions and from an established breast carcinoma cell line (18). In an elegant study, human mammary epithelial cells were used to generate non-adherent spheroids (designated mammospheres) in cell culture and demonstrate the presence of the three mammary cell lineages. More importantly, the cells in the mammospheres were clonally derived, providing evidence for a single pluripotent stem cell (19). However, the true role of stem cells in cancer in general has been less elucidated. In order to shed more light specifically on interactions of normal stem cells and cancer stem cells as a possible mechanism of cancer initiation and progression, the current design of our study was selected. Although an experimental model is never completely consistent with the complex mechanisms in nature, our results support the concept that cancer stem cells initiate the tumor and the interaction with regular tissue-resident stem cells contribute to tumor growth.

Studies from Dr Chia-Cheng Chang's group clearly demonstrate that there exist breast adult stem cells residing in the breast tissue that are capable of differentiating into breast tissue and to give rise to breast carcinoma cells (53–62). These breast adult stem cells express Oct4 (17) and have the ability to differentiate into other cell types and to form budding/ductal structures on Matrigel (63). More interestingly, these cells are more susceptible to telomerase activation (63) and immortalization by SV40 large T antigen (59). Using complementary DNA microarray analysis, 148 genes have been identified as being either upregulated or downregulated related to immortalization (64). These studies provided enhanced understanding of breast stem cell and tumor initiation.

Limitations

Otsu *et al.* investigated on the effect of bone marrow-derived stem cells on angiogenesis in an *in vitro* Matrigel angiogenesis assay and an *in vivo* melanoma model. They found concentration-dependent inhibition of angiogenesis by mesenchymal stem cells. Therefore, future studies should try different condition for a general phenomenon (65).

Supplementary materials

Supplementary Table 1 and Figures 1–4 can be found at http://carcin.oxfordjournals.org/

Funding

This research was supported by the Department of Defense Breast Cancer Research Program W81XWH-08-1-0523 01 (to YHS) and by Alliance of Cardiovascular Researchers (to EA).

Acknowledgements

Conflict of Interest Statement: None declared.

References

1. Bhowmick,N.A. *et al*. (2004) Stromal fibroblasts in cancer initiation and progression. *Nature*, **432**, 332–337.
2. Olumi,A.F. *et al*. (1999) Carcinoma-associated fibroblasts direct tumor progression of initiated human prostatic epithelium. *Cancer Res.*, **59**, 5002–5011.
3. Cornil,I. *et al*. (1991) Fibroblast cell interactions with human melanoma cells affect tumor cell growth as a function of tumor progression. *Proc. Natl Acad. Sci. USA*, **88**, 6028–6032.
4. Karnoub,A.E. *et al*. (2007) Mesenchymal stem cells within tumour stroma promote breast cancer metastasis. *Nature*, **449**, 557–563.
5. Sappino,A.P. *et al*. (1988) Smooth-muscle differentiation in stromal cells of malignant and non-malignant breast tissues. *Int. J. Cancer*, **41**, 707–712.
6. De Wever,O. *et al*. (2003) Role of tissue stroma in cancer cell invasion. *J. Pathol.*, **200**, 429–447.
7. Ronnov-Jessen,L. *et al*. (1995) The origin of the myofibroblasts in breast cancer. Recapitulation of tumor environment in culture unravels diversity and implicates converted fibroblasts and recruited smooth muscle cells. *J. Clin. Invest.*, **95**, 859–873.
8. Chauhan,H. *et al*. (2003) There is more than one kind of myofibroblast: analysis of CD34 expression in benign, *in situ*, and invasive breast lesions. *J. Clin. Pathol.*, **56**, 271–276.
9. Ishii,G. *et al*. (2003) Bone-marrow-derived myofibroblasts contribute to the cancer-induced stromal reaction. *Biochem. Biophys. Res. Commun.*, **309**, 232–240.
10. Zuk,P.A. *et al*. (2001) Multilineage cells from human adipose tissue: implications for cell-based therapies. *Tissue Eng.*, **7**, 211–228.
11. Altman,A.M. *et al*. (2008) Dermal matrix as a carrier for *in vivo* delivery of human adipose-derived stem cells. *Biomaterials*, **29**, 1431–1442.
12. Sadat,S. *et al*. (2007) The cardioprotective effect of mesenchymal stem cells is mediated by IGF-I and VEGF. *Biochem. Biophys. Res. Commun.*, **363**, 674–679.
13. Bai,X. *et al*. (2007) Electrophysiological properties of human adipose tissue-derived stem cells. *Am. J. Physiol. Cell Physiol.*, **293**, C1539–C1550.
14. Bai,X. *et al.* (2007) VEGF receptor Flk-1 plays an important role in c-kit expression in adipose tissue derived stem cells. *FEBS Lett.*, **581**, 4681–4684.
15. Altman,A.M. *et al*. (2008) IFATS Series: human adipose-derived stem cells seeded on a silk fibroin-chitosan scaffold enhance wound repair in a murine soft tissue injury model. *Stem Cells,* in press.
16. Dontu,G. *et al*. (2003) *In vitro* propagation and transcriptional profiling of human mammary stem/progenitor cells. *Genes Dev.*, **17**, 1253–1270.
17. Tai,M.H. *et al*. (2005) Oct4 expression in adult human stem cells: evidence in support of the stem cell theory of carcinogenesis. *Carcinogenesis*, **26**, 495–502.
18. Ponti,D. *et al*. (2005) Isolation and *in vitro* propagation of tumorigenic breast cancer cells with stem/progenitor cell properties. *Cancer Res.*, **65**, 5506–5511.
19. Dontu,G. *et al*. (2003) Stem cells in normal breast development and breast cancer. *Cell Prolif.*, **36** (suppl. 1), 59–72.
20. Zuk,P.A. *et al*. (2002) Human adipose tissue is a source of multipotent stem cells. *Mol. Biol. Cell*, **13**, 4279–4295.
21. Halvorsen,Y.D. *et al*. (2001) Thiazolidinediones and glucocorticoids synergistically induce differentiation of human adipose tissue stromal cells: biochemical, cellular, and molecular analysis. *Metabolism*, **50**, 407–413.
22. Sen,A. *et al*. (2001) Adipogenic potential of human adipose derived stromal cells from multiple donors is heterogeneous. *J. Cell. Biochem.*, **81**, 312–319.
23. Erickson,G.R. *et al*. (2002) Chondrogenic potential of adipose tissue-derived stromal cells *in vitro* and *in vivo*. *Biochem. Biophys. Res. Commun.*, **290**, 763–769.

24. Wickham,M.Q. *et al*. (2003) Multipotent stromal cells derived from the infrapatellar fat pad of the knee. *Clin. Orthop. Relat. Res.*, **412**, 196–212.
25. Kilroy,G.E. *et al*. (2007) Cytokine profile of human adipose-derived stem cells: expression of angiogenic, hematopoietic, and pro-inflammatory factors. *J. Cell. Physiol.*, **212**, 702–709.
26. Corre,J. *et al*. (2006) Human subcutaneous adipose cells support complete differentiation but not self-renewal of hematopoietic progenitors. *J. Cell. Physiol.*, **208**, 282–288.
27. Seo,M.J. *et al*. (2005) Differentiation of human adipose stromal cells into hepatic lineage *in vitro* and *in vivo*. *Biochem. Biophys. Res. Commun.*, **328**, 258–264.
28. Talens-Visconti,R. *et al*. (2007) Human mesenchymal stem cells from adipose tissue: differentiation into hepatic lineage. *Toxicol. In Vitro*, **21**, 324–329.
29. Safford,K.M. *et al*. (2002) Neurogenic differentiation of murine and human adipose-derived stromal cells. *Biochem. Biophys. Res. Commun.*, **294**, 371–379.
30. Kang,S.K. *et al*. (2004) Neurogenesis of Rhesus adipose stromal cells. *J. Cell Sci.*, **117**, 4289–4299.
31. Krampera,M. *et al*. (2007) Induction of neural-like differentiation in human mesenchymal stem cells derived from bone marrow, fat, spleen and thymus. *Bone*, **40**, 382–390.
32. Halvorsen,Y.C. *et al*. (2000) Adipose-derived stromal cells—their utility and potential in bone formation. *Int. J. Obes. Relat. Metab. Disord.*, **24** (suppl. 4), S41–S44.
33. Huang,J.I. *et al*. (2002) Rat extramedullary adipose tissue as a source of osteochondrogenic progenitor cells. *Plast. Reconstr. Surg.*, **109**, 1033–1041; (discussion 1042–1043).
34. Timper,K. *et al*. (2006) Human adipose tissue-derived mesenchymal stem cells differentiate into insulin, somatostatin, and glucagon expressing cells. *Biochem. Biophys. Res. Commun.*, **341**, 1135–1140.
35. Lee,J.H. *et al*. (2006) Human adipose-derived stem cells display myogenic potential and perturbed function in hypoxic conditions. *Biochem. Biophys. Res. Commun.*, **341**, 882–888.
36. Schimrosczyk,K. *et al*. (2008) Liposome-mediated transfection with extract from neonatal rat cardiomyocytes induces transdifferentiation of human adipose-derived stem cells into cardiomyocytes. *Scand. J. Clin. Lab. Invest.*, **68**, 464–472.
37. Orimo,A. *et al*. (2005) Stromal fibroblasts present in invasive human breast carcinomas promote tumor growth and angiogenesis through elevated SDF-1/CXCL12 secretion. *Cell*, **121**, 335–348.
38. Iyengar,P. *et al*. (2003) Adipocyte-secreted factors synergistically promote mammary tumorigenesis through induction of anti-apoptotic transcriptional programs and proto-oncogene stabilization. *Oncogene*, **22**, 6408–6423.
39. Manabe,Y. *et al*. (2003) Mature adipocytes, but not preadipocytes, promote the growth of breast carcinoma cells in collagen gel matrix culture through cancer-stromal cell interactions. *J. Pathol.*, **201**, 221–228.
40. Zannettino,A.C. *et al*. (2008) Multipotential human adipose-derived stromal stem cells exhibit a perivascular phenotype *in vitro* and *in vivo*. *J. Cell. Physiol.*, **214**, 413–421.
41. Strieter,R.M. *et al*. (2004) CXC chemokines in angiogenesis of cancer. *Semin. Cancer Biol.*, **14**, 195–200.
42. Ohira,S. *et al*. (2006) Possible regulation of migration of intrahepatic cholangiocarcinoma cells by interaction of CXCR4 expressed in carcinoma cells with tumor necrosis factor-alpha and stromal-derived factor-1 released in stroma. *Am. J. Pathol.*, **168**, 1155–1168.
43. Kollmar,O. *et al*. (2007) Stromal cell-derived factor-1 promotes cell migration and tumor growth of colorectal metastasis. *Neoplasia*, **9**, 862–870.
44. Brand,S. *et al*. (2005) CXCR4 and CXCL12 are inversely expressed in colorectal cancer cells and modulate cancer cell migration, invasion and MMP-9 activation. *Exp. Cell Res.*, **310**, 117–130.
45. Mishra,P.J. *et al*. (2008) Carcinoma-associated fibroblast-like differentiation of human mesenchymal stem cells. *Cancer Res*, **68**, 4331–4339.
46. Balkwill,F. (2004) Cancer and the chemokine network. *Nat. Rev. Cancer*, **4**, 540–550.
47. Darash-Yahana,M. *et al*. (2004) Role of high expression levels of CXCR4 in tumor growth, vascularization, and metastasis. *FASEB J.*, **18**, 1240–1242.
48. Smith,M.C. *et al*. (2004) CXCR4 regulates growth of both primary and metastatic breast cancer. *Cancer Res.*, **64**, 8604–8612.
49. Rubin,J.B. *et al*. (2003) A small-molecule antagonist of CXCR4 inhibits intracranial growth of primary brain tumors. *Proc. Natl Acad. Sci. USA*, **100**, 13513–13518.
50. Goldman,E. (1907) The growth of malignant disease in man and the lower animals with special reference to the vascular system. *Lancet*, **2**, 1236–1240.
51. Folkman,J. (2003) Fundamental concepts of the angiogenic process. *Curr. Mol. Med.*, **3**, 643–651.
52. Miranville,A. *et al*. (2004) Improvement of postnatal neovascularization by human adipose tissue-derived stem cells. *Circulation*, **110**, 349–355.
53. Kao,C.Y. *et al*. (1995) Two types of normal human breast epithelial cells derived from reduction mammoplasty: phenotypic characterization and response to SV40 transfection. *Carcinogenesis*, **16**, 531–538.
54. Kao,C.Y. *et al*. (1997) Growth requirements and neoplastic transformation of two types of normal human breast epithelial cells derived from reduction mammoplasty. *In Vitro Cell. Dev. Biol. Anim.*, **33**, 282–288.
55. Kang,K.S. *et al*. (1997) Expression of estrogen receptors in a normal human breast epithelial cell type with luminal and stem cell characteristics and its neoplastically transformed cell lines. *Carcinogenesis*, **18**, 251–257.
56. Kang,K.S. *et al*. (1998) Involvement of tyrosine phosphorylation of p185(c-erbB2/neu) in tumorigenicity induced by X-rays and the neu oncogene in human breast epithelial cells. *Mol. Carcinog.*, **21**, 225–233.
57. Hsieh,C.Y. *et al*. (1999) Stem cell differentiation and reduction as a potential mechanism for chemoprevention of breast cancer. *Chinese Pharm. J.*, **51**, 15–30.
58. Chang,C.C. *et al*. (2000) Roles of ionizing radiation in neoplastic transformation of human breast epithelial cells. In Moriarty,M., Mothersill,C., Seymour,C., Edington,M., Ward,J.F. and Fry,R.J.M. (eds.). *Radiation Research*. Vol. II, pp. 576–579.
59. Chang,C.C. *et al*. (2001) A human breast epithelial cell type with stem cell characteristics as target cells for carcinogenesis. *Radiat. Res.*, **155**, 201–207.
60. Chang,C.C. (2006) Recent translational research: stem cells as the roots of breast cancer. *Breast Cancer Res.*, **8**, 103.
61. De Flora,S. *et al*. (2006) Induction by 7,12-dimethylbenz(a)anthracene of molecular and biochemical alterations in transformed human mammary epithelial stem cells, and protection by N-acetylcysteine. *Int. J. Oncol.*, **29**, 521–529.
62. Ahn,E.H. *et al*. (2006) Evaluation of sphinganine and sphingosine as human breast cancer chemotherapeutic and chemopreventive agents. *Exp. Biol. Med. (Maywood)*, **231**, 1664–1672.
63. Sun,W. *et al*. (1999) High susceptibility of a human breast epithelial cell type with stem cell characteristics to telomerase activation and immortalization. *Cancer Res.*, **59**, 6118–6123.
64. Park,J.S. *et al*. (2004) Gene expression analysis in SV40-immortalized human breast luminal epithelial cells with stem cell characteristics using a cDNA microarray. *Int. J. Oncol.*, **24**, 1545–1558.
65. Otsu,K. *et al*. (2008) Concentration dependent inhibition of angiogenesis by mesenchymal stem cells. *Blood*, in press.

Received November 17, 2008; revised January 21, 2009; accepted January 24, 2009